


 Cite this: *RSC Adv.*, 2026, 16, 11937

## Periodic acid-promoted methylenation of imidazoheteroarenes: a green approach using ethylene glycol as a C1 source

 Marcelo S. Franco,<sup>†a</sup> Matheus Y. G. Watanabe,<sup>†a</sup> Jhefferson S. Guilhermi,<sup>b</sup> Bruno S. Souza,<sup>b</sup> Sumbal Saba,<sup>id</sup>\*<sup>b</sup> Jamal Rafique,<sup>id</sup>\*<sup>bc</sup> and Antonio L. Braga<sup>id</sup>\*<sup>a</sup>

Herein, we describe an environmentally sustainable methodology for the methylenation of C3(sp<sup>2</sup>) imidazoheteroarenes, employing formaldehyde (C1) generated *in situ* via oxidative cleavage of ethylene glycol—a renewable feedstock. The protocol utilizes water as a non-toxic solvent and stoichiometric reagents, aligning with green chemistry principles by ensuring high atomic economy and minimal waste. Optimized conditions enable regioselective bis-heterocycle formation with yields up to 97%. The reaction proceeds through a Malaprade oxidation-mediated ionic pathway mediated by 0.5 molar equiv. of periodic acid, and demonstrates broad substrate scope, including imidazo[1,2-*a*]pyridines and imidazo[2,1-*b*]thiazoles. Scalability was validated (70% yield at 5.5 mmol scale), highlighting its potential for industrial applications. This method offers a robust, metal-free alternative for C–H functionalization.

Received 23rd December 2025

Accepted 29th January 2026

DOI: 10.1039/d5ra09947a

[rsc.li/rsc-advances](https://rsc.li/rsc-advances)

Nitrogen-containing heterocycles represent a major field of study in organic chemistry.<sup>1</sup> Research in this area is extensive, driven by the significant physiological and pharmacological properties of N-heterocyclic compounds.<sup>2,3</sup> They serve as fundamental building blocks for many biologically important molecules, including vitamins, nucleic acids, and pharmaceuticals.<sup>1–3</sup> Their broad applicability stems from their ability to act as proton donors or acceptors and to engage in diverse non-covalent interactions, such as hydrogen bonding, van der Waals forces, hydrophobic effects, and  $\pi$ -stacking.<sup>4</sup>

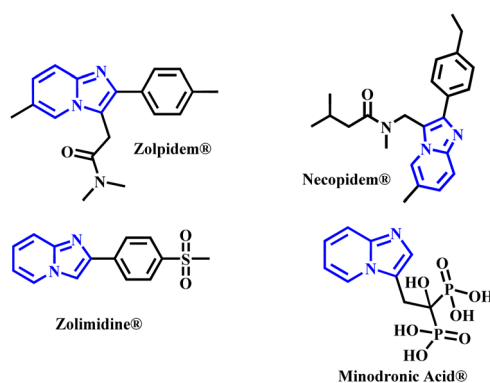
Vitaku, Smith, and Njardarson (2014) published a comprehensive analysis of the structural diversity, substitution patterns, and frequency of nitrogen-containing heterocycles in US FDA-approved drugs. Their work highlights the relevance of these structures, which range from active components in therapeutic agents to key building blocks for new drug candidates.<sup>5</sup>

In recent decades, numerous methods have been developed for the construction and functionalization of imidazoheterocycles.<sup>6</sup> Among these, imidazo[1,2-*a*]pyridine (IP) is particularly prominent. This scaffold is present in many commercial drugs, such as Zolpidem®, Necopidem®, Zolimidine®, and Minodronic acid® (Fig. 1), making it an important core structure

with a wide range of structural variations.<sup>7</sup> Furthermore, IP derivatives possess significant luminescent properties,<sup>8–12</sup> and are also employed as fluorescent sensors for metal ions,<sup>9,13</sup> and in phosphorescent complexes for light-emitting devices.<sup>14</sup>

In organic synthesis, ethylene glycol is known as a valuable two-carbon (C2) synthon but it can also be strategically cleaved to function as a C1 source for the construction of various one-carbon functional groups. Under appropriate conditions, the C–C bond of ethylene glycol can be cleaved, to generate formaldehyde *in situ*.<sup>15</sup> The released formaldehyde can then be trapped *in situ* to form methylene bridges or incorporate into heterocycles.<sup>16</sup>

Over recent decades, several research groups have developed methods for the functionalization of the C–H bonds in IPs. Most of these methods focus on the nucleophilic C-3 position. The


 Fig. 1 Imidazo[1,2-*a*]pyridine (IP) containing commercialized drugs.

<sup>a</sup>Departamento de Química, Universidade Federal de Santa Catarina, Florianópolis, 88040-900, Santa Catarina, Brazil. E-mail: braga.antonio@ufsc.br

<sup>b</sup>Laboratory of Sustainable Synthesis and Organochalcogen (LabSO), Instituto de Química, Universidade Federal de Goiás – UFG, Goiânia, 74690-900, Goiás, Brazil. E-mail: sumbalsaba@ufg.br

<sup>c</sup>Instituto de Química, Universidade Federal do Mato Grosso do Sul – UFMS, Campo Grande, 79074-460, Mato Grosso do Sul, Brazil. E-mail: jamal.rafique@ufms.br

<sup>†</sup> These authors contributed equally to this work.

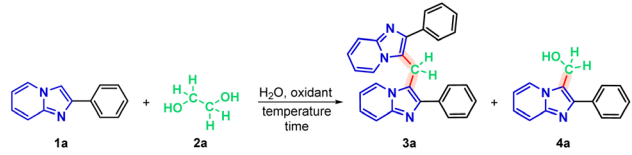

ability to achieve this selective functionalization without needing to protect the C-3 site is particularly advantageous from a synthetic perspective.<sup>7</sup> Consequently, one important functionalization of IPs is methylenation (Scheme 1). The insertion of a methylene group into a molecule is a highly attractive synthetic strategy for constructing complex structures, especially bis-heterocyclic systems.<sup>17</sup>

As part of our research interest in designing and developing sustainable processes, as well as the C(sp<sup>2</sup>)-H functionalization of biologically-relevant heteroarenes,<sup>18,19</sup> herein, we describe, a regioselective and environmentally benign protocol for the methylenation *via* Malaprade oxidation. Based on the interest in creating new, more sustainable synthetic routes for IP derivatives.

In the first part of the new protocol, studies were carried out to optimize the reaction conditions using 2-phenylimidazo[1,2-*a*]pyridine (**1a**) (0.3 mmol), ethylene glycol (**2a**) (1 molar equivalent) and 0.5 mL of distilled water. As expected, the reaction does not occur without the presence of an oxidizing agent, for 1 h at 100 °C (Table 1, entry 1). Therefore, an attempt was made to find an oxidizing agent, testing iodic acid (HIO<sub>3</sub>), sodium iodide (NaIO<sub>3</sub>) and potassium iodide (KIO<sub>3</sub>), keeping the other conditions constant. However, reactions did not occur (entries 2, 3 and 4, respectively). The addition of periodic acid proved to be efficient as an oxidizing agent for the system, obtaining 73% of the 2-phenylimidazo[1,2-*a*]pyridine dimer (**3a**) and 24% of the hydroxymethylated IP (**4a**) (entry 5).

In order to increase the yield of the dimer, a reduction of 1 molar equivalent to 0.5 of reagent **2a** was performed to make it more chemoselective, proving to be efficient, since the yield was increased from 73% to 79% of the desired product (**3a**) and, reduced from 24% to 7% of the by-product (**4a**) (entry 6). When

Table 1 Optimization of reaction conditions<sup>a</sup>



Entry	2a (equiv.)	Oxidant (equiv.)	Temperature (°C)	Time (h)	Yield <sup>b</sup> (%)	
					3a	4a
1	1	—	100	1	—	—
2	1	HIO <sub>3</sub> (1)	100	1	—	—
3	1	NaIO <sub>3</sub> (1)	100	1	—	—
4	1	KIO <sub>3</sub> (1)	100	1	—	—
5	1	H <sub>5</sub> IO <sub>6</sub> (1)	100	1	73	24
6	0.5	H <sub>5</sub> IO <sub>6</sub> (0.5)	100	1	79	7
7	0.4	H <sub>5</sub> IO <sub>6</sub> (0.4)	100	1	69	8
8	0.5	H <sub>5</sub> IO <sub>6</sub> (0.5)	110	1	88	5
9	0.5	H <sub>5</sub> IO <sub>6</sub> (0.5)	120	1	95	n.d.
10	0.5	H <sub>5</sub> IO <sub>6</sub> (0.5)	120	0.5	62	14

<sup>a</sup> Conditions: **1a** (0.3 mmol), **2a** (molar equivalent), oxidant (molar equivalent), H<sub>2</sub>O (0.5 mL), time (hour), temperature (°C). —: no reaction. —: absence. n.d.: not detected. <sup>b</sup> Isolated yield.

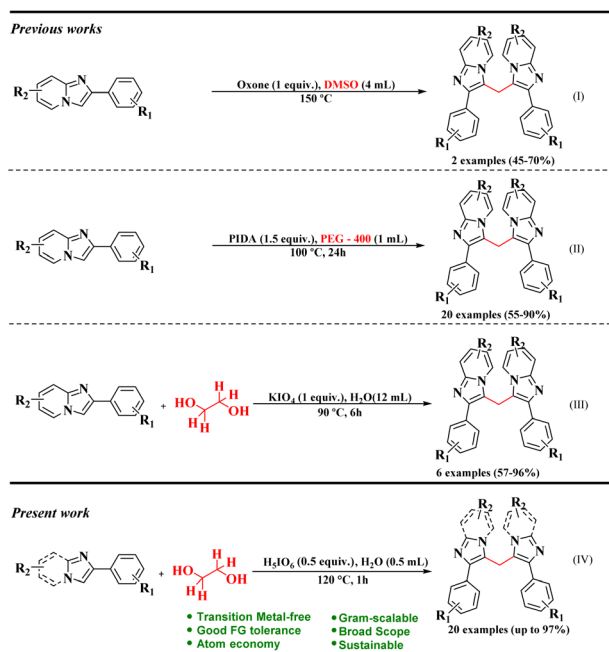
the reduction was performed to 0.4 molar equivalent of **2a**, a reduction to 69% of the dimer (**3a**) and to 8% of the alcohol of 2-phenylimidazo[1,2-*a*]pyridine (**4a**) was observed (entry 7).

The next modification performed was the temperature, testing at 110 °C and 120 °C, obtaining, respectively, excellent values of 88% for the dimer (**3a**) and 5% for the alcohol (**4a**) (entry 8); and only the dimer (**3a**) in 95% yield (entry 9).

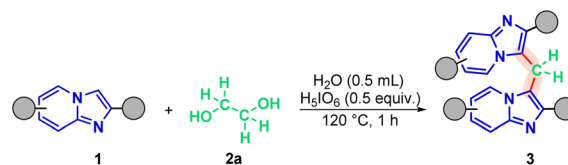
Finally, we tried to optimize the reaction time, reducing it to 30 min (entry 10), which proved to be inefficient compared to the best condition, entry 9, since with the shortest time, 62% of the desired dimer (**3a**) and 14% of the hydroxymethylated by-product (**4a**).

With the optimal reaction conditions established (Scheme 2), we applied the optimized methodology to a series of substrates derived from IPs to evaluate the generality of the new protocol.

When donating groups were attached to the pyridine nucleus of the 2-phenylimidazo[1,2-*a*]pyridine scaffold, the corresponding products (**3b–3d**, **3n**) were isolated in excellent yields of 76–97%. A similar monosubstituted system with an electron-



Scheme 1 Methylenation reactions in literature.



Scheme 2 Optimized protocol of methylenation of imidazo[1,2-*a*]pyridine **1**. Conditions: **1** (0.3 mmol), **2a** (0.5 molar equivalent), H<sub>5</sub>IO<sub>6</sub> (0.5 equiv.), H<sub>2</sub>O (0.5 mL), time (1 h), temperature (120 °C).



withdrawing group (**3i**) was also synthesized, albeit in a lower yield of 53% (Fig. 2).

The influence of substituents on the pendant phenyl group was also investigated. Electron-donating groups (**1e**, **1f**) provided high yields (84–87%) of **3e** and **3f**. Conversely, electron-withdrawing groups (**1g**, **1h**, **1j–1o**) resulted in a broader yield range of 55–87% for products **3g**, **3h**, **3j–3n** (Fig. 2). The reaction of the unsubstituted IP precursor proceeded with low efficiency, yielding only 36% of **3o**. This lower yield could be due to the lack of the stabilizing aryl substituent that is present in all other substrates (**3a–3n**).

To prove the versatility of the method, the protocol was applied to other N-heteroarene nuclei, such as imidazo[2,1-*b*]thiazole **1A** (Scheme 3).

In general, the desired products **4a–d** were obtained in good to excellent yields. When evaluating the compounds, the influence of electronic effects is notable. Compounds with electron-withdrawing groups linked to the phenyl ring, such as **4d** and **4e**, presented yields in the range of 58–63%. In contrast, the compound with an electron-donating group, **4c**, presented a significantly higher yield of 89% (Fig. 3).

To evaluate the method's variability compared to other sources of methylene groups, reactions were performed using glycerol (**2b**) and PEG-400 (**2c**). The reaction with glycerol gave a 92% yield, while the one with PEG-400 gave only 8% (Table 2).

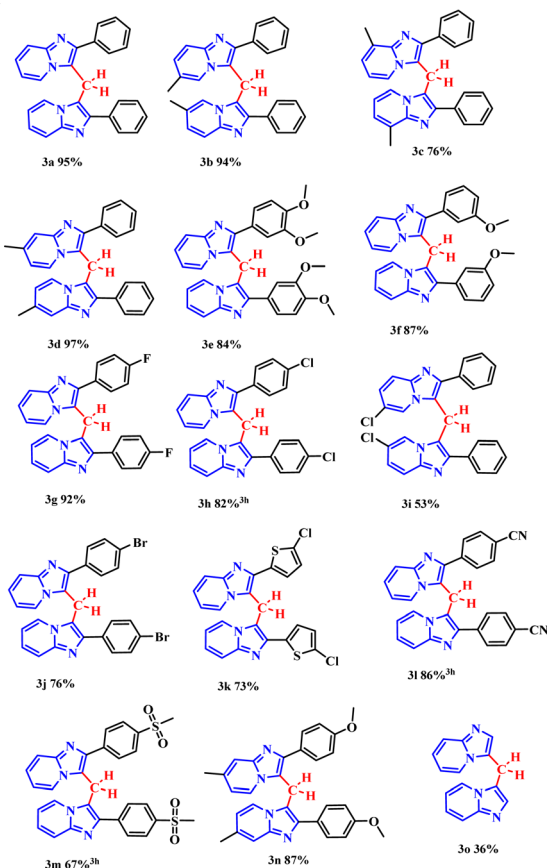
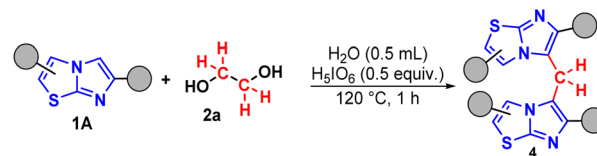


Fig. 2 Scope of imidazo[1,2-*a*]pyridine.



Scheme 3 Optimized protocol of methylenation of imidazo[2,1-*b*]thiazole **1A**. Conditions: **1A** (0.3 mmol), **2a** (0.5 molar equivalent),  $H_5IO_6$  (0.5 equiv.),  $H_2O$  (0.5 mL), time (1 h), temperature (120 °C).

In the next step, a scale-up experiment was performed using 5.5 mmol of **1a**, ethylene glycol (2.75 mmol, 0.5 equiv.), and periodic acid ( $H_5IO_6$ , 2.75 mmol, 0.5 equiv.) in water (10 mL). The reaction mixture was heated at 120 °C for 6 hours, as a longer reaction time was anticipated to be necessary for the increased scale. The desired product (**3a**) was obtained in 70% yield (0.7738 g), demonstrating that the method can accommodate variations in scale.

In order to elucidate the mechanism by which the dimer formation reaction takes place, the mechanism of the methylenation reaction was examined. By adding TEMPO to the standard experiment conditions, product **3a** was obtained in 92% yield (Table 3, entry 1), suggesting that the reaction occurs *via* an ionic pathway. The experiment was also carried out under an argon atmosphere (Table 3, entry 2), obtaining 93% yield, verifying that  $O_2$  does not have an active role in the reaction mechanism.

To confirm the proposed mechanism, the reaction was performed under optimized conditions by replacing ethylene glycol (**2a**) with formaldehyde (**5a**), a known source of methylene carbon (Table 4, entry 1). The successful formation of the dimer proved that formaldehyde generated *in situ* from the Malaprade reaction reacts with **1a**.

This hypothesis was further supported using (2-phenylimidazo[1,2-*a*]pyridin-3-yl)methanol (**5b**) under the same optimized conditions (Table 4, entry 2). The high yield obtained strongly suggests that **5b** is a key reaction intermediate.

To elucidate the role of periodic acid, the reaction with alcohol **5b** was repeated without the oxidant (Table 4, entry 3).

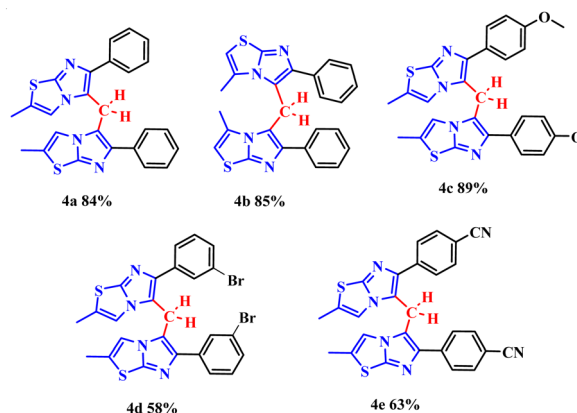


Fig. 3 Scope of imidazo[2,1-*b*]thiazoles.



Table 2 Methylene group source experiments<sup>a</sup>

Entry	Methylene group source	3a, yield <sup>b</sup> (%)
1	<b>2b</b> (glycerol) 	93%
2	<b>2c</b> (PEG <sub>400</sub> ) 	8%

<sup>a</sup> Conditions: **1a** (0.3 mmol), **2** (molar equivalent), H<sub>5</sub>IO<sub>6</sub> (0.5 molar equivalent), H<sub>2</sub>O (0.5 mL), time (1 h), temperature (120 °C). <sup>b</sup> Isolated yield.

Table 3 Control experiments<sup>a</sup>

Entry	Control experiments	3a, yield <sup>b</sup> (%)
1	<b>Tempo</b> 	92%
2	Argon (Ar)	93%

<sup>a</sup> Conditions: **1a** (0.3 mmol), **2** (0.15 mmol), H<sub>5</sub>IO<sub>6</sub> (0.5 molar equivalent), H<sub>2</sub>O (0.5 mL), time (1 h), temperature (120 °C). <sup>b</sup> Isolated yield.

No product was formed, confirming that an oxidizing agent is essential, even when starting from the proposed intermediate.

The importance of water as the solvent was also investigated. The reaction was conducted without water, using a three-fold excess of ethylene glycol (**2a**) to act as both reagent and solvent. Only trace amounts of product **3a** were detected by TLC. The isolated quantity was insufficient for quantitative analysis or characterization by NMR.

Collectively, these results reinforce the reaction mechanism proposed by Franco.<sup>17b</sup> It begins with the *in situ* formation of formaldehyde (**5a**) *via* oxidative cleavage of ethylene glycol (**2a**) according to the Malaprade reaction. This is followed by the formation of the hydroxylated intermediate (**5b**), which subsequently undergoes nucleophilic attack to form the dimer.

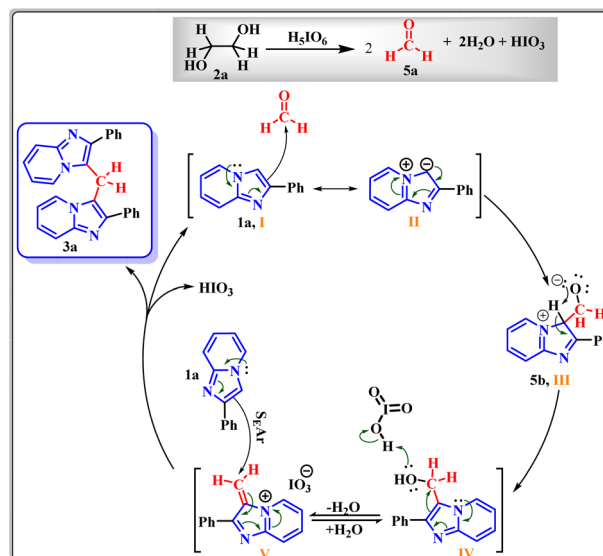
Based on all experimental evidence and previous reports, we propose a tentative mechanism for this transformation (Scheme 4). The mechanism begins with the Malaprade reaction, in which the 1,2-diol (**2a**) is cleaved by periodic acid to generate formaldehyde (**5a**) *in situ*, along with water and iodate. Formaldehyde (**5a**) then reacts with **1a** to form the intermediate (2-phenylimidazo[1,2-*a*]pyridin-3-yl)methanol, denoted as **III** (**5b**).

Table 4 Intermediary experiments<sup>a</sup>

Entry	Intermediary	Condition	3a, yield <sup>b</sup> (%)
1	<b>5a</b> 	—	92%
2	<b>5b</b> 	—	96%
3	<b>5b</b> 	Only H <sub>2</sub> O 120 °C, 1 h	0%

<sup>a</sup> Conditions: **1a** (0.3 mmol), **2** (molar equivalent), H<sub>5</sub>IO<sub>6</sub> (0.5 molar equivalent), H<sub>2</sub>O (0.5 mL), time (1 h), temperature (120 °C). <sup>b</sup> Isolated yield.

Subsequent dehydration of the protonated species (**IV**) yields the key electrophilic intermediate (**V**). Finally, nucleophilic attack by a second molecule of 2-phenylimidazo[1,2-*a*]pyridine (**1a**) on the methylene carbon of species **V** leads to the formation of the final product (**3a**).



Scheme 4 Mechanistic proposal.



## Conclusions

In this work, we developed a sustainable and efficient methodology for the methylenation of imidazoheteroarenes using ethylene glycol as a renewable and economical source of formaldehyde (C1), generated *in situ via* Malaprade oxidation. The protocol employs water as a non-toxic solvent, stoichiometric reagents, and mild reaction conditions, aligning with the principles of green chemistry. The method is highly regioselective, operationally simple, and delivers excellent yields (up to 97%) across a broad substrate scope, including imidazo[1,2-*a*]pyridines and imidazo[2,1-*b*]thiazoles. Mechanistic studies indicate an ionic pathway, with formaldehyde and a hydroxymethylated intermediate playing key role. Scalability was demonstrated (70% yield on gram-scale), highlighting the method's robustness for preparative applications.

This approach not only advances the synthetic toolbox for C–H functionalization of biologically relevant heterocycles but also underscores the potential of renewable feedstocks in sustainable chemistry. Future studies may unlock new pharmacological applications of these synthesized bis-heterocycles, leveraging the structural diversity enabled by this methodology.

## Author contributions

Conceptualization: M. S. F., S. S., J. R., and A. L. B.; methodology: M. S. F. and M. Y. G. W.; validation: M. S. F.; formal analysis: M. S. F., M. Y. G. W., I. M. O., and B. S. S.; investigation: M. S. F., M. Y. G. W., I. M. O., B. S. S., S. S., and J. R.; resources: S. S., J. R., and A. L. B.; data curation: M. S. F., M. Y. G. W., and I. M. O.; writing – original draft: M. S. F., and J. R.; writing – review and editing: S. S. and J. R.; visualization: S. S., J. R., and A. L. B.; supervision: S. S., J. R., and A. L. B.; project administration: S. S., J. R., and A. L. B.; funding acquisition: S. S., J. R., and A. L. B. All authors read and approved the final draft of the manuscript.

## Conflicts of interest

There are no conflicts to declare.

## Data availability

All experimental data supporting this article are available in the supplementary information (SI). Supplementary information: experimental procedures, substrates, general procedure for the preparation of compound **3** and **4**, characterization data, and NMR spectra. See DOI: <https://doi.org/10.1039/d5ra09947a>.

## Acknowledgements

We gratefully acknowledge CNPq, CAPES (Finance Code 001), and INCT-Catálise/CNPq/FAPESC for financial support and fellowships. M. S. F. is grateful to CNPq for the scholarship (142225/2017-7). J. R., and S. S. would like to acknowledge CNPq (308875/2026-5, 401355/2025-0, 316687/2023-5, 309975/2022-0, 404172/2023-7, 405655/2023-1). S. S., and J. R. also

acknowledges the following FAPEG public calls: Chamada Pública FAPEG/SES no. 18/2025 (ARB202519100003), Chamada Pública FAPEG no. 05/2025 (PVE2025041000055), and Chamada Pública FAPEG no. 21/2025 (PEE2025331000083 and PEE2025331000108).

## References

- 1 S. Roy, S. K. Das, H. Khatua, S. L. Das and B. Chattopadhyay, Road Map for the Construction of High-Valued N-Heterocycles via Denitrogenative Annulation, *Acc. Chem. Res.*, 2021, **54**, 4395–4409.
- 2 (a) L. M. Aroura, F. M. Alminderej, H. R. Alhumayln, A. H. Alsaimi, F. Medini, H. A. Mohammed, S. A. Almahmoud, R. A. Khan and N. H. Mekni, Benzimidazole(s): synthons, bioactive lead structures, total synthesis, and the profiling of major bioactive categories, *RSC Adv.*, 2025, **15**, 7571–7608; (b) N. Dey, A. Mandal, R. Jana, A. Bera, S. A. Azad, S. Giri, M. Iqbal and S. Samanta, Recent developments in the solvent-free synthesis of heterocycles, *New J. Chem.*, 2023, **47**, 13035–13079; (c) R. Javahershensas, J. Han, M. Kazemi and P. J. Jervis, Recent Advances in the Multicomponent Synthesis of Heterocycles using Thiosemicarbazide, *ChemistrySelect*, 2024, **9**, e202401496; (d) J. Rafique, G. Farias, S. Saba, E. Zapp, I. C. Belletini, C. A. Momoli Salla, I. H. Bechtold, M. R. Scheide, J. S. Santos Neto, D. Monteiro de Souza Junior, H. de Campos Braga, L. F. B. Ribeiro, F. Gastaldon, C. T. P. Pich and T. E. A. Frizon, Selenylated-oxadiazoles as promising DNA intercalators: Synthesis, electronic structure, DNA interaction and cleavage, *Dyes Pigment.*, 2020, **180**, 108519.
- 3 (a) X. Yang, Z. Jiao, C. Fan, W. Ye, S. Lv, X. Wang, C. Wang, K. Zhagn, X. Ke and W. Zhou, Macrocyclic Compounds: Unveiling Their Distinctive Antiviral Advantages in Medicinal Research, *J. Med. Chem.*, 2025, **68**, 21035–21071; (b) G. Ahmad, M. Sohail, M. Bilal, N. Rasool, M. U. Qamar, C. Ciurea, L. G. Marceanu and C. Misarca, N-Heterocycles as Promising Antiviral Agents: A Comprehensive Overview, *Molecules*, 2024, **29**, 2232; (c) D. Dhara, L. A. Mulard and M. Hollenstein, Natural, modified and conjugated carbohydrates in nucleic acids, *Chem. Soc. Rev.*, 2025, **54**, 2948–2983; (d) M. Godoy-Gallardo, M. Merino-Gomez, L. C. Matiz, M. A. Mateso-Timoneda, F. J. Gil and R. A. Perez, Nucleoside-Based Supramolecular Hydrogels: From Synthesis and Structural Properties to Biomedical and Tissue Engineering Applications, *ACS Biomater. Sci. Eng.*, 2023, **9**(1), 40–61; (e) C. M. Marhall, J. G. Federice, C. N. Bell, P. B. Cox and J. T. Njardarson, An Update on the Nitrogen Heterocycle Compositions and Properties of U.S. FDA-Approved Pharmaceuticals (2013–2023), *J. Med. Chem.*, 2024, **67**, 11622–11655.
- 4 N. Kerru, L. Gummini, S. Maddila, K. K. Gngu and S. B. Jonnalagadda, A Review on Recent Advances in Nitrogen-Containing Molecules and Their Biological Applications, *Molecules*, 2020, **25**, 1909.



- 5 E. Vitaku, D. T. Smith and J. T. Njardarson, Analysis of the Structural Diversity, Substitution Patterns, and Frequency of Nitrogen Heterocycles among U.S. FDA Approved Pharmaceuticals: Miniperspective, *J. Med. Chem.*, 2014, **57**, 10257–10274.
- 6 (a) A. K. Bagdi, S. Santra, K. Monir and A. Hajra, Synthesis of imidazo[1,2-*a*]pyridines: a decade update, *Chem. Commun.*, 2015, **51**, 1555–1575; (b) J. A. Tali, G. Kumar, B. K. Sharma, Y. Rasool, Y. Sharma and R. Shankar, Synthesis and site selective C–H functionalization of imidazo-[1,2-*a*]pyridines, *Org. Biomol. Chem.*, 2023, **21**, 7267–7289; (c) J. Rafique, S. Saba, M. S. Franco, L. Bettanin, A. R. Schneider, L. T. Silva and A. L. Braga, Direct, Metal-free C(sp<sup>2</sup>)-H Chalcogenation of Indoles and Imidazopyridines with Dichalcogenides Catalysed by KIO<sub>3</sub>, *Chem.–Eur. J.*, 2018, **24**, 4173; (d) S. Saba, C. R. Dos Santos, B. R. Zavarise, A. A. S. Naujorks, M. S. Franco, A. R. Schneider, M. R. Scheide, R. F. Affeldt, J. Rafique and A. L. Braga, Photoinduced, Direct C(sp<sup>2</sup>)-H Bond Azo Coupling of Imidazoheteroarenes and Imidazoanilines with Aryl Diazonium Salts Catalyzed by Eosin Y, *Chem.–Eur. J.*, 2020, **26**, 4461–4466; (e) S. Saba, J. Rafique, M. S. Franco, A. R. Schneider, L. Espíndola, D. O. Silva and A. L. Braga, Rose Bengal Catalysed Photo-Induced Selenylation of Indoles, Imidazoles And Arenes: A Metal Free Approach, *Org. Biomol. Chem.*, 2018, **16**, 880–885; (f) J. Rafique, S. Saba, A. R. Rosário and A. L. Braga, Regioselective, Solvent- and Metal-Free Chalcogenation of Imidazo[1,2-*a*]pyridines by Employing I<sub>2</sub>/DMSO as the Catalytic Oxidation System, *Chem.–Eur. J.*, 2016, **22**, 11854–11862.
- 7 (a) G. T. Burkner, D. A. Dias, K. F. S. d. Souza, A. J. P. d. Araújo, D. C. L. S. Basilio, F. T. Jacobsen, A. C. R. d. Moraes, S. E. Silva-Filho, M. F. d. O. Cavalcante, C. A. d. O. Moraes, S. Saba, M. L. R. Macedo, E. J. Paredes-Gamero, J. Rafique and E. B. Parisotto, Selenylated Imidazo [1,2-*a*]pyridine Induces Cell Senescence and Oxidative Stress in Chronic Myeloid Leukemia Cells, *Molecules*, 2023, **28**, 893; (b) D. C. dos Santos, J. Rafique, S. Saba, G. M. Almeida, T. Siminski, C. Pádua, D. W. Filho, A. Zamoner, A. L. Braga, R. C. Pedrosa and F. Ourique, Apoptosis oxidative damage-mediated and antiproliferative effect of selenylated imidazo[1,2-*a*]pyridines on hepatocellular carcinoma HepG2 cells and in vivo, *J. Biochem. Mol. Toxicol.*, 2020, **35**, e22663; (c) D. C. dos Santos, J. Rafique, S. Saba, V. M. A. S. Grinevicius, D. W. Filho, A. Zamoner, A. L. Braga, R. C. Pedrosa and F. Ourique, IP-Se-06, a Selenylated Imidazo[1,2-*a*]pyridine, Modulates Intracellular Redox State and Causes Akt/mTOR/HIF-1 $\alpha$  and MAPK Signaling Inhibition, Promoting Antiproliferative Effect and Apoptosis in Glioblastoma Cells, *Oxid. Med. Cell. Longevity*, 2022, **2022**, 3710449; (d) I. C. Veloso, E. Delanogare, A. E. Machado, S. P. Braga, G. K. Rosa, A. F. de Bem, J. Rafique, S. Saba, R. N. da Trindade, F. Z. Galetto and E. L. G. Moreira, A selanylimidazopyridine (3-SePh-IP) reverses the prodepressant- and anxiogenic-like effects of a high-fat/high-fructose diet in mice, *J. Pharm. Pharmacol.*, 2021, **73**, 673–681.
- 8 R. Salim, E. Ech-chihbi, H. Oudda, E. F. Hajjaji, M. Taleb and S. Jodeh, A Review on the Assessment of Imidazo[1,2-*a*]pyridines As Corrosion Inhibitor of Metals, *J. Bio Tribo Corros.*, 2019, **5**, 14.
- 9 A. Douhal, F. Amat-Guerri and A. U. Acuña, Probing Nanocavities with Proton-Transfer Fluorescence, *Angew. Chem., Int. Ed. Engl.*, 1997, **36**, 1514–1516.
- 10 T. Mutai, H. Tomoda, T. Ohkawa, Y. Yabe and K. Araki, Switching of polymorph-dependent ESIPT luminescence of an imidazo[1,2-*a*]pyridine derivative, *Angew. Chem., Int. Ed.*, 2008, **47**, 9522–9524.
- 11 T. Mutai, H. Sawatani, T. Shida, H. Shono and K. Araki, Tuning of excited-state intramolecular proton transfer (ESIPT) fluorescence of imidazo[1,2-*a*]pyridine in rigid matrices by substitution effect, *J. Org. Chem.*, 2013, **78**(6), 2482–2489.
- 12 S. Furukawa, H. Shono, T. Mutai and K. Araki, Colorless, transparent, dye-doped polymer films exhibiting tunable luminescence color: controlling the dual-color luminescence of 2-(2'-hydroxyphenyl)imidazo[1,2-*a*]pyridine derivatives with the surrounding matrix, *ACS Appl. Mater. Interfaces*, 2014, **6**, 16065–16070.
- 13 S. Xiao, Z. Liu, J. Zhao, M. Pei, G. Zhang and W. He, A novel fluorescent sensor based on imidazo[1,2-*a*]pyridine for Zn<sup>2+</sup>, *RSC Adv.*, 2016, **6**, 27119–27125.
- 14 S. Takizawa, J. Nishida, T. Tsuzuki, S. Tokito and Y. Yamashita, Phosphorescent Iridium complexes based on 2-Phenylimidazo[1,2-*a*]pyridine ligands: tuning of emission color toward the blue region and application to polymer light-emitting devices, *Inorg. Chem.*, 2007, **46**, 4308–4319.
- 15 (a) H. Yue, Y. Zhao, X. Ma and J. Gong, Ethylene glycol: properties, synthesis, and applications, *Chem. Soc. Rev.*, 2012, **41**, 4218–4244; (b) G. H. Schenk, Periodate cleavage of glycols: A quantitative organic analysis experiment, *J. Chem. Educ.*, 1962, **39**, 32; (c) A. Kołodziejczyk, M. Błaziak, K. Podgórnjak, A. Jezierska and K. Błaziak, The Malaprade reaction mechanism for ethylene glycol oxidation by periodic acid based on density functional theory (DFT), *Phys. Chem. Chem. Phys.*, 2023, **25**, 21448–21455.
- 16 (a) C. I. Attorresi, J. A. Ramirez and B. Westermann, Formaldehyde surrogates in multicomponent reactions, *Beilstein J. Org. Chem.*, 2025, **21**, 564–595; (b) A. Rodil, J. Deska and M. H. G. Preschtl, Formaldehyde and its surrogates as a C1 platform for defossilised modern societies, *Chem. Soc. Rev.*, 2025, **54**, 11398–11422.
- 17 (a) J. Kour, V. Venkateswarlu, P. K. Verma, Y. Hussain, G. Dubey, P. V. Bharatam, S. C. Sahoo and S. D. Sawant, Oxone-DMSO Triggered Methylene Insertion and C(sp<sup>2</sup>)-C(sp<sup>3</sup>)-H-C(sp<sup>2</sup>) Bond Formation to Access Functional Bis-Heterocycles, *J. Org. Chem.*, 2020, **85**, 4951–4962; (b) M. S. Franco, S. Saba, J. Rafique and A. L. Braga, KIO<sub>4</sub>-mediated Selective Hydroxymethylation/Methylenation of Imidazo-Heteroarenes: A Greener Approach, *Angew. Chem.*, 2021, **133**, 18602; (c) R. Kumar, D. Rawat and S. Adimurthy, Polyethylene Glycol (PEG-400) as Methylene



- Spacer and Green Solvent for the Synthesis of Heterodiarylmethanes under Metal-Free Conditions, *Eur. J. Org. Chem.*, 2020, 3499; (d) N. Vodnala, S. Singh and C. K. Hazara, Lewis Acid-Promoted Typical Friedel–Crafts Reactions Using DMSO as a Carbon Source, *J. Org. Chem.*, 2022, **87**, 10044–10053; (e) P. G. Dalai, S. Swain and N. Panda, DMSO–DCE Triggered Chemodivergent C-Methylenation of Electron-Rich Arenes: An Easy Access to Diarylmethanes, *J. Org. Chem.*, 2024, **89**(4), 2599–2604; (f) S. Thunga, M. Inapanui, N. Singh and H. P. Koktala, Rongalite as a Methylene Surrogate: Synthesis of Heterodiarylmethanes via C(sp<sup>2</sup>)-H Functionalization, *J. Org. Chem.*, 2024, **89**(24), 18313–18321.
- 18 (a) B. L. Tornquist, G. de Paula Bueno, J. C. M. Willig, I. M. de Oliveira, H. A. Stefani, J. Rafique, S. Saba, B. A. Iglesias, G. V. Botteselle and F. Manarin, *ChemistrySelect*, 2018, **3**, 6358; (b) M. Godoi, G. V. Botteselle, J. Rafique, M. S. T. Rocha, J. M. Pena and A. L. Braga, Solvent-free Fmoc protection of amines under microwave irradiation, *Asian J. Org. Chem.*, 2013, **2**, 746–749; (c) A. A. O. Moraes, R. B. C. Santos, M. F. O. Cavalcante, J. S. Guilhermi, M. A. Ali, G. V. Botteselle, T. E. A. Frizon, M. I. A. Shah, L. M. Lião, A. Beatriz, S. Saba and J. Rafique, Urea Hydrogen Peroxide and Ethyl Lactate, an Eco-Friendly Combo System in the Direct C(sp<sup>2</sup>)-H Bond Selenylation of Imidazo[2,1-*b*]thiazole and Related Structures, *ACS Omega*, 2023, **8**, 39535–39545; (d) G. V. Botteselle, W. C. Elias, L. Bettanin, R. F. S. Canto, D. N. O. Salin, F. A. R. Barbosa, S. Saba, H. Gallardo, G. Ciancaleoni, J. B. Domingos, J. Rafique and A. L. Braga, Catalytic Antioxidant Activity of Bis-Aniline-Derived Diselenides as GPx Mimics, *Molecules*, 2021, **26**, 4446.
- 19 (a) M. S. T. Rocha, J. Rafique, S. Saba, J. B. Azeredo, D. Back, M. Godoi and A. L. Braga, Regioselective hydrothiolation of terminal acetylene catalyzed by magnetite (Fe<sub>3</sub>O<sub>4</sub>) nanoparticles, *Synth. Commun.*, 2017, **47**, 291–298; (b) J. R. L. Sousa, M. S. Franco, L. D. Mendes, L. A. Araujo, J. S. S. Neto, T. E. A. Frizon, V. B. Dos Santos, E. Carasek, S. Saba, J. Rafique and A. L. Braga, KIO<sub>3</sub>-catalyzed selective oxidation of thiols to disulfides in water under ambient conditions, *Org. Biomol. Chem.*, 2024, **22**, 2175; (c) M. Haroon, M. Khalid, K. Shahzadi, T. Akhtar, S. Saba, J. Rafique, S. Ali, M. Irfan, M. M. Alam and M. Imran, Alkyl 2-(2-(arylidene)alkylhydrazinyl)thiazole-4-carboxylates: Synthesis, acetyl cholinesterase inhibition and docking studies, *J. Mol. Struct.*, 2021, **1245**, 131063.

